# Room-temperature *p*-induced surface ferromagnetism: First-principles study

Guntram Fischer,[1] Nadiezhda Sanchez,[2] Waheed Adeagbo,[1] Martin Lüders,[3] Zdzislawa Szotek,[3] Walter M. Temmerman,[3] Arthur Ernst,[4] Wolfram Hergert,[1] and M. Carmen Muñoz[2]

[1]*Institut für Physik, Martin-Luther-Universität Halle-Wittenberg, Von-Seckendorff-Platz 1, D-06120 Halle, Germany*

[2]*Instituto de Ciencia de Materiales de Madrid, Consejo Superior de Investigaciones Científicas, Cantoblanco, E-28049 Madrid, Spain*

[3]*Daresbury Laboratory, Daresbury, Warrington, WA4 4AD, United Kingdom*

[4]*Max-Planck-Institut für Mikrostrukturphysik, Weinberg 2, D-06120 Halle, Germany*

(Received 6 October 2011; published 11 November 2011)

We prove a spontaneous magnetization of the oxygen-terminated ZnO (0001) surface by utilizing a multicode, SIESTA and KKR, first-principles approach, involving both LSDA+$U$ and self-interaction corrections to treat electron correlation effects. Critical temperatures are estimated from Monte Carlo simulations, showing that at and above 300 K the surface is thermodynamically stable and ferromagnetic. The observed half-metallicity and long-range magnetic order originate from the presence of $p$ holes in the valence band of the oxide. The mechanism is universal in ionic oxides and points to a new route for the design of ferromagnetic low-dimensional systems.

DOI: 10.1103/PhysRevB.84.205306 PACS number(s): 75.70.Rf, 73.20.−r, 75.50.Pp, 81.05.Zx

## I. INTRODUCTION

Since the first report of magnetism in Co-doped ZnO,[1] spontaneous magnetization persistent above room temperature (RT) has been found in a number of dilute magnetic oxides, even for materials containing no transition-metal impurities. The presence of ferromagnetism (FM) without magnetic elements has been revealed in thin films and nanoparticles of undoped $HfO_2$, ZnO, MgO, $SnO_2$, $TiO_2$, or $SrTiO_3$,[2–4] among others. The measured FM in undoped, otherwise diamagnetic, bulk oxides presents several general and distinct characteristics, such as a Curie temperature ($T_C$) substantially above room temperature, small coercive fields, and a similar dependence of the coercive field and remanent magnetization on temperature.[4] This universality indicates a common origin. However, despite the intense research, the physical origin of the magnetic ordering and, therefore, its control remains a controversial unresolved problem.[5–7] It was shown theoretically that localized holes in bulk oxides can lead to local moments and a half-metallic behavior.[8] However, a high $T_C$ requires defect concentrations incompatible with the stability of the material. Furthermore, the necessary large strength and long range of the defect-defect magnetic interaction is inconsistent with the actual localization of defect orbitals in ionic oxides.[9]

In an alternative approach, which some of us proposed a few years ago, FM is induced at the surface due to its intrinsic characteristics: breakdown of symmetry, unsaturated bonds, or uncompensated ionic charges.[10,11] The physical mechanism underlying the spontaneous magnetization of the surface relies on the formation of holes at the top of the oxygen-derived $p$-like minority valence band (VB) of the oxide. This mechanism is analogous to that responsible for cation vacancies[12] or acceptor doping[13] induced magnetism. Both defects and surfaces impose boundary conditions that give rise to the uncompensated charges leading to magnetization. However, surface states, although confined to the topmost layers, are usually extended in two dimensions[14] and, thus, the subtle interplay between localization and extended states, which is required for the moment formation and strong and long-range magnetic order, can be reached more easily at surfaces. In addition, there is growing experimental evidence that the FM signal is mostly concentrated in the near-surface region, grain boundaries, or nanostructure interfaces.[4,15]

Here we report a multicode first-principles study of surface-induced FM in ZnO, considered as the prototype of a high-temperature FM oxide. We observe a spontaneous magnetization of the O-terminated ZnO (0001) surface when the oxygen atoms occupy the fcc threefold coordinated sites, as shown in Fig. 1. The magnetic interaction between spin moments is strong and the calculated Curie temperature is $\gtrsim$300 K.The surface is thermodynamically stable in a significant range of oxygen pressures. The presence of oxygen atoms in extended local areas of the (0001) surface has been experimentally reported either in rough surfaces with incomplete O terminations[16] or in ordered structures[17] and has been suggested to be a stabilization mechanism of the (0001) surface with Zn polarity.[18]

The present paper is structured as follows. Section II describes the numerical procedure of the multicode approach used and gives the respective details. The results of these investigations are presented and discussed in Sec. III and briefly summarized in Sec. IV.

## II. NUMERICAL APPROACH

### A. Methods

In our calculations ZnO surfaces were modeled by periodically repeated slabs separated by a vacuum region. To facilitate a more adequate treatment of electron correlations and $p$ bands containing holes,[9,19,20] we employed two approaches. First, the LSDA+$U$ method, as implemented in the pseudopotential SIESTA code,[21] known to well reproduce the ground state of bulk ZnO, and, second, the local self-interaction corrections (LSIC), as implemented in the multiple scattering theory, the LSIC-KKR code.[23] While the electronic structure and structural relaxations were performed with SIESTA, the magnetic interactions for the relaxed structures were investigated with the LSIC-KKR code. In the latter, after determining the SIC ground state, the system was mapped onto a Heisenberg

 

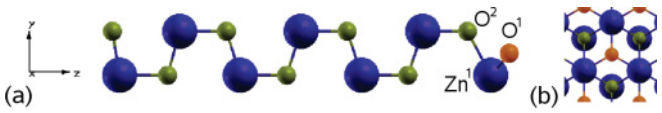


FIG. 1. (Color) (a) Investigated ZnO slab unit cell (vacuum region not shown) in its ground-state structure after relaxation, with oxygen (small yellow and orange) and zinc (big blue) atoms. The $(000\bar{1})$ surface is on the left end and the (0001) on the right. The latter is characterized by the topmost O atom in the threefold coordinated hollow position, $O^1$, and the Zn and O atom underneath, labeled $Zn^1$ and $O^2$, respectively. (b) Top view of the (0001) surface.

Hamiltonian $H = -\sum_{ij} J_{ij}\mathbf{e}_i \cdot \mathbf{e}_j - \sum_i \Delta_i (e_i^z)^2$ by calculating the real space magnetic interaction parameters $J_{ij}$, where $i$ and $j$ stand for atomic sites, via the magnetic force theorem (MFT).[24] $\Delta_i$ is the magnetic anisotropy energy at site $i$, and here was treated as a parameter in Monte Carlo (MC) simulations performed to estimate Curie temperatures.[25]

### B. Numerical details

In the SIESTA calculations, the basis sets were constituted by multiple-zeta polarized localized numerical atomic orbitals (AO); for Zn, we employed double-zeta (DZ) $s$ and $d$ AOs plus a single-zeta (SZ) $p$ AO. For oxygen DZ $s$ and $p$ AOs plus a SZ $d$ AO were used. The empirical Coulomb $U =$ 5.7 eV and exchange $J = 1$ eV parameters were chosen to model the orbital dependent Hubbard-like potential for the Zn $d$ states.[26] We modeled the surfaces by a slab geometry, in which slabs containing between 15 and 17 atomic planes along the crystallographic wurtzite $c$ axis and separated by a vacuum region of at least 20 Å were repeated periodically. Reciprocal space integration was performed on a $12 \times 12 \times 1$ Monkhorst-Pack supercell. Convergence in the $k$ mesh and the inclusion of relaxations were carefully checked due to their paramount importance for an accurate description of magnetism.

Dipolar corrections were applied for the asymmetric slabs. Bulklike behavior was always attained at the innermost central plane and the structure and electronic properties of the surfaces, both (0001) and $(000\bar{1})$, turned out to be independent of the symmetry of the slab. More details about the conditions of the calculations are found in Refs. 11,27, and 28.

For a more adequate description of the correlated electrons in the system, namely beyond that of local and semilocal approximations to density functional theory, the so-called local self-interaction correction (LSIC) approach, implemented within the framework of the multiple scattering Korringa-Kohn-Rostoker (KKR) method,[23] was employed to the relaxed (equilibrium) structures determined by SIESTA. As in the LSIC-KKR method, one deals with energy-dependent quantities, a complex energy contour of 24 Gaussian quadrature points was used in the calculations throughout, and for the Brillouin zone integrations a $12 \times 12 \times 2$ $k$-points mesh was constructed. The crystal potential was constructed in the atomic sphere approximation. So-called empty spheres were used to improve space filling. As mentioned above, the LSIC-KKR determined ground-state electronic structure was also used to investigate the magnetic interactions of the studied surfaces by applying the MFT. For this, we used the same complex energy contour of 24 points; convergence of the $J_{ij}$ with respect to the number of $k$ points was achieved with a $12 \times 12 \times 2k$-points mesh per energy point for the first 18 of them, and a $30 \times 30 \times 5$ $k$ mesh for the last six energy points, lying close to the Fermi energy.

The MC simulations were performed by constructing lattices of 3200 to 4608 sites representing the two magnetic oxygen atoms. Importance sampling was done using the Metropolis algorithm. During the simulations, the system was relaxed into equilibrium at a temperature $T$ above $T_C$. Then $T$ was gradually reduced. At each $T$ point, the system was assumed to have reached equilibrium after 20 000 MC steps, after which measuring the observables and averaging over further 20 000 MC steps was done. $T_C$ was obtained by inspecting the graphs of the susceptibility $\chi$, the specific heat $C_V$, and the so-called Binder cumulant $U_4$. All three quantities deliver the same values for $T_C$. Further details about the $J_{ij}$ calculations via the MFT and the MC simulations are given in Ref. 29.

## III. RESULTS AND DISCUSSION

### A. Geometrical structure

Using SIESTA, the calculated in-plane $a = 3.25$ Å and out-of-plane $c = 5.20$ Å lattice parameters of ZnO turned out to be in good agreement with the experimental values,[30] and we obtained a band gap of 1.25 eV. The O-ZnO $(000\bar{1})$ surface presents a compression of the O-Zn bond of ≈4% and a smaller relaxation of the next two layers. Contrary to this, at the (0001) surface the O-Zn bond length is 2.04 Å, which is slightly larger than the 1.98 Å of bulk bonds, although the large variations occur for the underneath bonds due to the outward relaxation of Zn atoms. The Zn-O pair distances, which present opposite relaxation, are 2.11 Å and 1.93 Å in the second and third layers, respectively. Subsequent layers retain their bulk structure.

Because of the symmetry of the ZnO crystal, Zn and O planes alternate along the [0001] direction and, due to the lack of inversion symmetry of the wurtzite structure, the polar (0001) and $(000\bar{1})$ ZnO surfaces are inequivalent. Several positions of the surface oxygen atoms were considered, including off-symmetric sites. We found that the O-ZnO $(000\bar{1})$ surface is stable and corresponds simply to the cleaved ZnO bulk crystal. The VB of the surface oxygen is not entirely filled; hence surface layers are metallic and exhibit partly occupied flat surface states at the top of the VB,[11] although the number of holes is small, about 0.14 electrons. For the O-terminated (0001) surface, however, the most stable configuration turns out to be the one with oxygen in the threefold fcc hollow site, as reported before.[18] This rearrangement of the top oxygen atom decreases the surface energy dramatically by ≈1 eV per O atom with respect to that of the cleaved cutoff crystal. The surface energy is even about 0.65 eV smaller than the formation energy of a Zn vacancy in bulk ZnO. The relaxed unit cell structure is illustrated in Fig. 1. The topmost oxygen atoms in both surfaces are threefold coordinated, and the O-Zn distances are slightly compressed and relaxed in the $(000\bar{1})$ and (0001) surfaces, respectively (see Supplemental Material[22]).

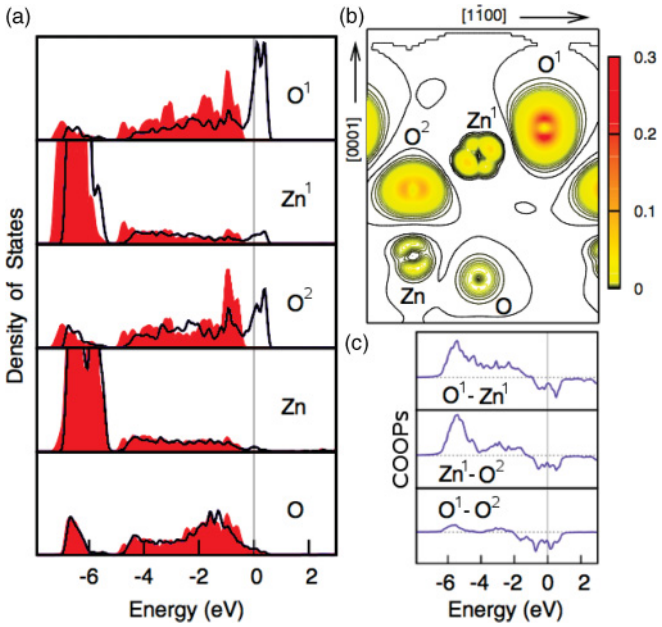


FIG. 2. (Color) (a) Spin-resolved LDOS of the topmost layers of the O-ended (0001)-h surface. Red filled (black) values represent majority (minority) spin states. (b) Spin-density distribution of the (0001)-h surface. (c) COOPs between the atoms in the first three layers. Energies are relative to $E_F$.

### B. Electronic structure

The layer resolved density of states (LDOS) corresponding to the (0001) surface is displayed in Fig. 2(a). The main features of the calculated LDOS reflect spin polarization and half-metallicity of the surface and the presence of the oxygen split-off band, with the Fermi level crossing the minority O band. The exchange splitting is large, having a magnitude of approximately 1.5 eV, and the narrowing of the minority bandwidth is particularly pronounced at the surface layer. The total magnetic moment (MM) is $\approx$1.5 $\mu_B$, corresponding to the induced number of holes, and the spin densities displayed in Fig. 2(b) confirm the surface localization of the magnetic moments.

The crystal orbital overlap populations (COOP) determine the wave function overlap of any two atoms and, therefore, their values can be related to their hybridization.[27] Thus the COOP between the atoms close to the surface, shown in Fig. 2(c), reveal a large hybridization between adjacent layers and evidence the extended character of states at the surface. Even the wave function overlap between $O^1$ and $O^2$ is noticeable, which is due to their short distance, 2.30 versus 3.25 Å for O atoms in the same plane.

The Mulliken charge differences and induced magnetic moments for the surface layers are given in Table I. It shows that there is a charge rearrangement at the topmost atomic layers, more pronounced in the surface oxygen, which sustains more than 60% of the induced $p$ holes. The orbital charge distribution is compatible with the spatial symmetry and the larger number of holes localized in the $p_z$ orbital (see Supplemental Material[22]). The nominal Mulliken population for bulk ZnO is already reached at three bilayers below the surface.

TABLE I. Layer resolved Mulliken charge differences[31] (in units of $e$)[31] and magnetic moments (in $\mu_B$) for the topmost layers of the (0001) surface. The layers are labeled according to Fig. 1.

| | $O^1$ | $Zn^1$ | $O^2$ |
|---|---|---|---|
| $\Delta Q$ | −0.38 | −0.01 | −0.19 |
| MM (SIESTA) | 0.94 | 0.01 | 0.53 |
| MM (LSIC-KKR) | 1.06 | −0.06 | 0.42 |

The surface-induced $p$ holes give rise to an open-shell configuration of the oxygen, which promotes the observed spontaneous spin polarization of the surface, analogously to the well-known paramagnetism of the $O_2$ molecule. Therefore, the half-metallicity of the ground state implies that surface magnetism is due to Hund's rule exchange, and electrons occupy orbitals in the open shell so as to maximize their total spin. The alignment of spins forming a symmetric spin state reduces the interaction energy. Therefore, whenever the energy gain from spin splitting of the oxygen-derived VB exceeds the energy loss in kinetic energy, it is advantageous for the system to spin polarize. The COOPs displayed in Fig. 2(c) substantiate this conclusion. Since they represent the overlap of the wave function of the surface atoms, they clearly show that the states have itinerant character, and thus the delocalization necessary for the magnetic coupling.

As the coordination number is reduced at the surface and the narrow oxygen $p$ band only partially filled, it is crucial to investigate also the degree of $p$ electron localization and its importance for an adequate description of correlation effects. This was accomplished with the LSIC-KKR method for the relaxed surface (see Supplemental Material[22]). The global SIC energy minimum was found for the scenario where, in addition to all the Zn 3$d$ electron states, all the majority, but no minority, $p$ electrons of $O^1$ benefit from localization and hence self-interaction correction. The resulting electronic structure confirms that the exchange splitting is confined to the topmost oxygen sites ($O^1$ and $O^2$) and the top of the valence band, as shown in Fig. 2(a). In Table I, we show that the calculated MM on $O^1$ is increased due to the increased localization of the majority $p$ band, causing an increased negative magnetization in the vicinity of the surface, with the half-metallicity preserved at the surface. The fact that the majority $p$ states of $O^2$ do not benefit from localization suggests that its MM is induced by $O^1$ through hybridization effects.

### C. Magnetic interaction

The exchange constants $J_{ij}$ for the above SIC ground state, calculated in the MFT approach, are presented in in Fig. 3. First, one sees that they are strongly ferromagnetic. Furthermore, the relevant contribution arises from interaction between $O^1$-$O^1$ and $O^1$-$O^2$ pairs. The reason for the very large nearest-neighbor coupling between $O^1$ and $O^2$ is the already mentioned close distance between these two atoms. The weak interaction between the $O^2$ atoms strengthens the assumption that the MM on them is induced by $O^1$ rather than being localized there. Figure 3 shows also that the $J_{ij}$'s have a similar behavior to such found for other half-metallic systems,[32,33] i.e.,

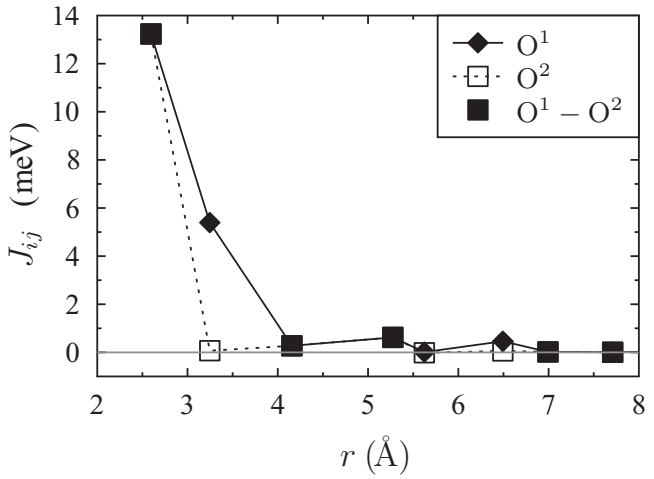


FIG. 3. $J_{ij}$ of pairs containing $O^1$ (♦) or $O^2$ (□), respectively, depending on the distance. The full black squares (■) mark the $J_{ij}$ between one $O^1$ and one $O^2$ atom.

they oscillate and decay relatively quickly. This means that the interaction is provided by the delocalized electrons.

For the MC simulations, the anisotropy $\Delta_i$ was assumed to be the same at $O^1$ and $O^2$ and was, as mentioned before, treated as a parameter. Choosing $\Delta = 0.1, 0.3, 1.0$, and 3.0 eV, the respective critical temperatures come out to be larger than room temperature at $T_C = 302$, 304, 320, and 346 K, with an error of ≈6 K (15 K for $\Delta = 0.1$ eV due to a broad transition). These results demonstrate that correlation corrections, applied to magnetic oxygen $p$ states, do not result in the collapse of magnetic interaction, unlike observed in bulk systems with point defects.[9]

### D. Relation to experiment

As mentioned before, several reports reveal the presence of oxygen atoms in ZnO(0001) surfaces, either in ordered structures or in extended O-terminated islands. Therefore, the O-ZnO(0001) surface with O in the threefold hollow site is a good candidate to explain the experimentally observed FM in thin layers and nanoparticles of ZnO.[3] Consequently, the magnetic ordering is restricted to a small fraction of atoms located in the vicinity of the surface, which justifies the low magnetization measured.[3,4]

Since the described magnetization mechanism requires partially filled $p$ states and is, therefore, not material specific, it represents a possible explanation to the large number of observations of magnetism in thin films and nanoparticles of formally nonmagnetic materials.[3] This is supported experimentally by the observed surface contribution to the ferromagnetic hysteresis loop of common diamagnetic oxide crystals[4] and also by a critical analysis of a large amount of published data for FM in Mn-doped and pure ZnO, which strongly suggests that grain boundaries are the intrinsic origin for RT FM.[15] In addition, similar magnetic behavior of polar surfaces has been found experimentally for diamond[34] and, theoretically, for oxides.[10]

Since FM is predicted in polar surfaces, it must be related to their stabilization mechanisms. Although usually their stabilization is explained in terms of ion removal or adsorption of charged molecules, it is still an open question and recently there has been evidence of electronic reconstruction and the formation of a two-dimensional electron gas with exotic properties at the surfaces and interfaces of ionic oxides.[14,35,36] Therefore, spontaneous magnetization could also be a plausible general stabilization mechanism of polar ionic surfaces.

## IV. SUMMARY

In conclusion, by combining density functional theory-based and MC methods, we have predicted ferromagnetism at the oxygen-terminated polar (0001) surface of ZnO with a $T_C$ of $\gtrsim$300 K. The spontaneous magnetization of the surface originates from the presence of $p$ holes in the minority valence band of the oxide, which renders a half-metallic surface. Spin polarization is enhanced through the bandwidth reduction associated with the surface, which drives moment formation more efficiently. In addition, surface states, although confined to the topmost layers, are extended in two dimensions and thus the subtle interplay between localization and extended states required for the development of long-range magnetic order can be reached at the surface. The mechanism is universal in ionic oxides, provided that the localization of the $p$ holes is strong enough for the formation of the MM. This two-dimensional magnetic state at the surface points to a new route for the design of ferromagnetic low-dimensional systems.

## ACKNOWLEDGMENTS

This work has been partially supported by the Spanish Ministry of Science and Technology under Grant No. MAT2009-14578-C03-03, and by the German Research Foundation (DFG) within the SFB 762.

[1] K. Ueda, H. Tabata, and T. Kawai, Appl. Phys. Lett. **79**, 988 (2001).
[2] M. Venkatesan, C. B. Fitzgerald, and J. M. D. Coey, Nature (London) **430**, 630 (2004).
[3] A. Sundaresan and C. Rao, Solid State Commun. **149**, 1197 (2009).
[4] M. Khalid, A. Setzer, M. Ziese, P. Esquinazi, D. Spemann, A. Pöppl, and E. Goering, Phys. Rev. B **81**, 214414 (2010).
[5] M. Stoneham, J. Phys. Condens. Matter **22**, 074211 (2010).
[6] J. Coey, P. Stamenov, R. Gunning, M. Venkatesan, and K. Paul, New J. Phys. **12**, 053025 (2010).
[7] T. Dietl, Nat. Mater. **9**, 965 (2010).
[8] I. S. Elfimov, S. Yunoki, and G. A. Sawatzky, Phys. Rev. Lett. **89**, 216403 (2002).
[9] A. Zunger, S. Lany, and H. Raebiger, Physics **3**, 53 (2010).

[10]S. Gallego, J. I. Beltrán, J. Cerdá, and M. C. Muñoz, J. Phys. Condens. Matter **17**, L451 (2005).
[11]N. Sanchez, S. Gallego, and M. C. Muñoz, Phys. Rev. Lett. **101**, 067206 (2008).
[12]C. Das Pemmaraju and S. Sanvito, Phys. Rev. Lett. **94**, 217205 (2005).
[13]H. Pan, J. B. Yi, L. Shen, R. Q. Wu, J. H. Yang, J. Y. Lin, Y. P. Feng, J. Ding, L. H. Van, and J. H. Yin, Phys. Rev. Lett. **99**, 127201 (2007).
[14]A. F. Santander-Syro, O. Copie, T. Kondo, F. Fortuna, S. Pailhes, R. Weht, X. G. Qiu, F. Bertran, A. Nicolaou, A. Taleb-Ibrahimi, P. Le Fevre, G. Herranz, M. Bibes, N. Reyren, Y. Apertet, P. Lecoeur, A. Barthelemy, and M. J. Rozenberg, Nature (London) **469**, 189 (2011).
[15]B. B. Straumal, A. A. Mazilkin, S. G. Protasova, A. A. Myatiev, P. B. Straumal, G. Schütz, P. A. van Aken, E. Goering, and B. Baretzky, Phys. Rev. B **79**, 205206 (2009).
[16]H. Matsui and H. Tabata, Phys. Rev. B **75**, 014438 (2007).
[17]S. Torbrügge, F. Ostendorf, and M. Reichling, J. Phys. Chem. C **113**, 4909 (2009).
[18]G. Kresse, O. Dulub, and U. Diebold, Phys. Rev. B **68**, 245409 (2003).
[19]A. Droghetti, C. D. Pemmaraju, and S. Sanvito, Phys. Rev. B **78**, 140404 (2008).
[20]W. A. Adeagbo, G. Fischer, A. Ernst, and W. Hergert, J. Phys. Condens. Matter **22**, 436002 (2010).
[21]J. M. Soler, E. Artacho, J. D. Gale, A. García, J. Junquera, P. Ordejón, and D. Sánchez-Portal, J. Phys. Condens. Matter **14**, 2745 (2002).
[22]See Supplemental Material at http://link.aps.org/supplemental/10.1103/PhysRevB.84.205306 for additional information on the electronic structure and the thermodynamic stability of the surface.
[23]M. Lüders, A. Ernst, M. Däne, Z. Szotek, A. Svane, D. Ködderitzsch, W. Hergert, B. L. Gyorffy, and W. M. Temmerman, Phys. Rev. B **71**, 205109 (2005).
[24]A. Liechtenstein, M. Katsnelson, V. Antropov, and V. Gubanov, J. Magn. Magn. Mater. **67**, 65 (1987).
[25]Further details on the KKR calculations and the MC simulations are given in the Supplemental Material[22] and in Ref. 29. More details on the SIESTA calculations can be found in Refs. 11,22,27, and 28.
[26]M. Khalid, M. Ziese, A. Setzer, P. Esquinazi, M. Lorenz, H. Hochmuth, M. Grundmann, D. Spemann, T. Butz, G. Brauer, W. Anwand, G. Fischer, W. A. Adeagbo, W. Hergert, and A. Ernst, Phys. Rev. B **80**, 035331 (2009).
[27]J. I. Beltrán, S. Gallego, J. Cerdá, J. S. Moya, and M. C. Muñoz, Phys. Rev. B **68**, 075401 (2003).
[28]N. Sanchez, S. Gallego, J. Cerdá, and M. C. Muñoz, Phys. Rev. B **81**, 115301 (2010).
[29]G. Fischer, M. Däne, A. Ernst, P. Bruno, M. Lüders, Z. Szotek, W. Temmerman, and W. Hergert, Phys. Rev. B **80**, 014408 (2009).
[30]U. Özgür, Y. L. Alivov, C. Liu, A. Teke, M. Reshchikov, S. Dogan, V. Avrutin, S.-J. Cho, and H. Morko, J. Appl. Phys. **98**, 041301 (2005).
[31]Charge differences have been also estimated by a Bader population analysis based on a VASP calculation. The results agree well with the Mulliken analysis.
[32]E. Şaşoğlu, L. M. Sandratskii, P. Bruno, and I. Galanakis, Phys. Rev. B **72**, 184415 (2005).
[33]S. Picozzi, M. Ležaić, and S. Blügel, Phys. Status Solidi A **203**, 2738 (2006).
[34]D. E. Ramaker and F. L. Hutson, Solid State Commun. **63**, 335 (1987).
[35]A. Ohtomo and H. Y. Hwang, Nature (London) **427**, 423 (2004).
[36]A. Tsukazaki, S. Akasaka, K. Nakahara, Y. Ohno, H. Ohno, D. Maryenko, A. Ohtomo, and M. Kawasaki, Nat. Mater. **9**, 889 (2010).